

# Conceptual Design and Analysis of a Shrouded-Type Wind Turbine for Low Wind Speed Condition

Syed Nazim Syed Ahmad<sup>1</sup>, Nurhayati Rosly<sup>2\*</sup>

<sup>1</sup> Faculty of Mechanical and Manufacturing Engineering,  
Universiti Tun Hussein Onn Malaysia, 86400, MALAYSIA

<sup>2</sup> Aircraft System and Design Research (ASDR), Department of Aeronautical Engineering,  
Faculty of Mechanical and Manufacturing Engineering,  
Universiti Tun Hussein Onn Malaysia, 86400, MALAYSIA

\*Corresponding Author: [nurhayati@uthm.edu.my](mailto:nurhayati@uthm.edu.my)  
DOI: <https://doi.org/10.30880/paat.2025.05.01.002>

## Article Info

Received: 31 December 2024  
Accepted: 28 May 2025  
Available online: 30 June 2025

## Keywords

Shrouded wind turbine, horizontal axis wind turbine, tip speed ratio, power coefficient, and torque coefficient

## Abstract

Wind energy represents a valuable renewable resource with significant potential for electrical power generation. While conventional wind turbines have been well-developed for electricity generation, they suffer from reduced efficiency and limited power output in remote areas with low wind speeds (typically below 7 m/s), where wind energy extraction becomes economically unviable. The central research question addressed in this study is: Can shrouded wind turbine technology significantly improve power generation efficiency compared to conventional open rotor designs under low wind speed conditions? This study aimed to propose a conceptual design of a shrouded wind turbine and analyze its performance under low wind speed conditions ranging from 4 to 7 m/s. The proposed wind turbine's performance was analyzed through extensive computational fluid dynamics (CFD) simulations using ANSYS Fluent. Key performance parameters, including power coefficient ( $C_p$ ), tip speed ratio (TSR), velocity distribution, pressure characteristics, torque generation, and power output capabilities, were investigated. Results demonstrated that the shrouded wind turbine achieved higher  $C_p$  values at elevated tip speed ratios compared to conventional open rotor configurations. Specifically, the shrouded design generated 17.1% more power at 4 m/s and 5.0% more power at 7 m/s wind speeds. The shrouded configuration increased air velocity by 11.6% at 4 m/s and 7.5% at 7 m/s compared to the open rotor design, demonstrating enhanced wind energy capture efficiency in low wind speed environments.

## 1. Introduction

Wind turbines are devices that transform the kinetic energy of moving air into electrical energy [1]. The global adoption of wind turbines for power generation has increased dramatically as they reduce reliance on fossil fuels and greenhouse gas emissions [2]. Wind power provides a clean and environmentally sustainable energy source, unlike fossil fuels that release harmful substances into the atmosphere, or the radioactive wastes produced by nuclear power [3]. Conventional wind turbines face significant performance limitations in low wind speed regions below 7 m/s [4, 5], which constitute substantial portions of global land areas with potential wind energy resources [6]. In these regions, conventional turbines exhibit reduced efficiency, lower power generation, and poor economic viability. The fundamental challenge lies in developing wind turbine technologies that can effectively

harness wind energy at low velocities while maintaining cost-effectiveness [7]. While shrouded wind turbine technology has shown promise for enhanced performance [8], limited research has been conducted on optimizing shroud designs specifically for low wind speed conditions. Existing studies primarily focus on moderate- to high-wind-speed applications, leaving a knowledge gap in understanding shrouded turbine behavior under low-wind-speed scenarios [9].

This study aimed to address these limitations by developing a conceptual design of a shrouded wind turbine optimized for low wind speed conditions ranging from 4 to 7 m/s and conducting comprehensive computational fluid dynamics analysis to evaluate its aerodynamic performance characteristics. The research focused on comparing power generation efficiency between shrouded and conventional open rotor designs while investigating the effect of shroud configuration on air velocity enhancement and pressure distribution. Through extensive CFD simulations using ANSYS Fluent, the study examined critical performance parameters, including power coefficient, tip speed ratio, velocity distribution, pressure characteristics, torque generation, and power output capabilities, to determine the viability of shrouded wind turbine technology for low wind speed applications. Shrouded wind turbines increase the mass flow rate and velocity of air passing through the rotor by creating a venturi effect, thereby enhancing power generation [10]. Computational fluid dynamics represents the primary method for analyzing aerodynamic fluid flow characteristics associated with wind turbines [11]. The power coefficient indicates the efficiency of wind energy extraction from available kinetic energy through the rotor, making it a crucial parameter for evaluating wind turbine performance under varying operational conditions [12].

## 2. Methodology

This study employed a systematic methodology to design and evaluate a shrouded wind turbine optimized for low wind speed conditions (4–7 m/s). Computer-Aided Design (CAD) tools were utilized for geometric modeling, followed by comprehensive CFD analysis using ANSYS Fluent [13]. The methodology was structured to ensure accurate design development and reliable simulation results, enabling a comprehensive comparison between the shrouded wind turbine and a conventional open rotor configuration.

### 2.1 Geometry Modelling

The design process utilized SolidWorks 2022 to create a detailed three-dimensional model of the shrouded wind turbine. Key components included the rotor (comprising a hub and blades), the shroud, and the integrated assembly. The rotor diameter was set at 1.6 m, with blades extending 0.8 m from a 0.2 m diameter hub. The shroud was designed with an inlet diameter of 1.62 m, expanding to 2.0 m at the exit, and an overall length of 1.2 m. These dimensions were selected to optimize the Venturi effect, enhancing airflow acceleration through the rotor. Fig. 1 illustrates the complete shrouded wind turbine model in SolidWorks, highlighting the specified dimensions and assembly configuration. The geometry was exported in IGES format for compatibility with CFD software.



**Fig. 1** Shrouded wind turbine in SolidWorks (Dimensions: Shroud diameter 1.62–2.0m; Rotor diameter 1.6m, Blade length: 0.8m, Hub diameter: 0.2m, Overall shroud length: 1.2m)

### 2.2 CFD Simulation Setup

The aerodynamic performance of the shrouded wind turbine was analyzed using ANSYS Fluent, employing a robust CFD methodology based on established protocols for wind turbine analysis [15, 16]. The simulation adopted the Multiple Reference Frame (MRF) approach to model the rotational behavior of the turbine, a method validated for steady-state wind turbine studies [11, 17].

### 2.2.1 Computational Domain and Meshing

The CFD simulation approach followed established methodologies for wind turbine analysis [15, 16]. A numerical simulation was conducted using ANSYS Fluent to analyze the rotational behavior of the wind turbine. The methodology adopted the Multiple Reference Frame (MRF) approach, which has been validated in previous wind turbine studies for steady-state analysis [11, 17]. The three-dimensional wind turbine geometry was saved in IGES format and imported into ANSYS Design Modeler. The computational domain was established following the best practices recommended by researchers in [18], with the turbine positioned in both rotational and stationary regions. The cylindrical domain radius exceeded the turbine dimensions by a factor of 10 to minimize boundary effects, consistent with established CFD guidelines for wind turbine simulations [11]. Fig. 2(a) depicts the imported shrouded wind turbine geometry in ANSYS, showing the overall setup within the computational domain. Mesh generation followed structured multi-block meshing principles, with hexahedral elements and enhanced refinement adjacent to blade surfaces to accurately resolve boundary layer effects ( $y^+ \approx 1$ ), following best practices in Zhang et al. [19]. Figure 2(b) presents the generated mesh, illustrating the refinement zones and element distribution. The mesh independence study was conducted with grid sizes ranging from 2.5 million to 6.8 million elements, ensuring solution convergence with less than 1% variation in key parameters.

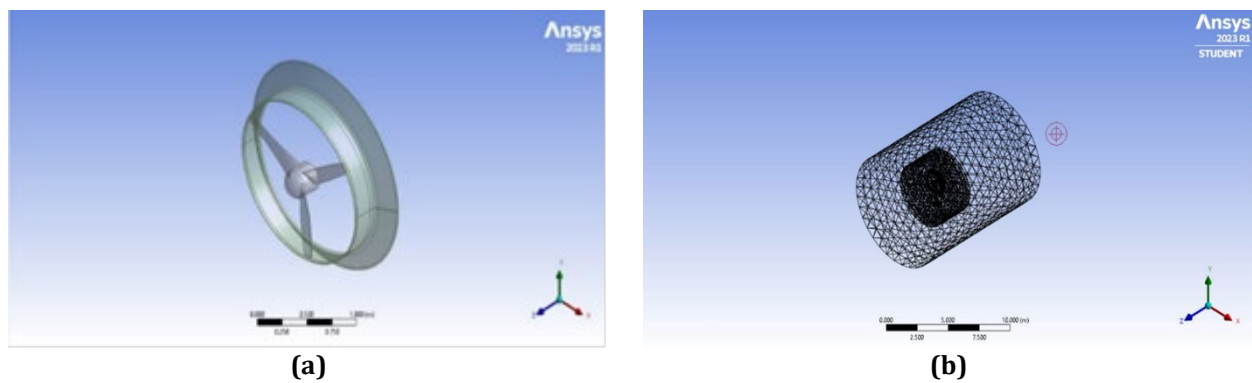


Fig. 2 (a) Shrouded wind turbine in Ansys; (b) Meshing generation

### 2.2.2 Simulation Parameters and Boundary Conditions

Simulations were conducted at wind speeds of 4 m/s and 7 m/s, representing typical low wind speed conditions prevalent in many geographical regions [20]. The turbulence model selection was based on comparative studies [11], which demonstrated the superior performance of the  $k-\omega$  SST model for wind turbine applications. The transient time, pressure-based solver, absolute velocity formulation, and overall setup were selected. In the meantime, the turbulent model flow used in this study is the  $k-\Omega$  (2 equation) (SST). The analysis setup and boundary conditions are included in Table 1:

Table 1 Parameters and boundary conditions

Parameters	Value
Wind speed	4 m/s & 7 m/s
Density	1.225 kg/m <sup>3</sup> (constant)
Viscosity	1.7894 × 10 <sup>-5</sup> m <sup>2</sup> /s (constant)
Gauge pressure	101.325 kPa (constant)
Temperature	288.15 K (constant)
Velocity Formulation	Absolute
Solver	Pressure-based
Time	Transient
Turbulence Model	$k-\omega$ (SST) – 2eqn
Material	Air
RPM	50
Slip Condition	None

### 3. Mathematical Formulation

The following mathematical equations were employed to calculate simulation results [21]:

Practical Power:

$$P_a = T\omega \quad (1)$$

Angular Velocity:

$$\omega = \frac{(TSR \times v)}{R} \quad (2)$$

Power Coefficient:

$$C_p = \frac{T\omega}{0.5\rho Av^3} \quad (3)$$

Power Generation:

$$P = 0.5\rho Av^3 C_p \quad (4)$$

where  $T$  is torque (N m),  $\omega$  is angular velocity (rad/s),  $TSR$  is the tip speed ratio,  $v$  is wind velocity (m/s), and  $R$  is the rotor radius (m),  $P$  is power output (W),  $\rho$  is air density (kg/m<sup>3</sup>), and  $A$  is the rotor swept area (m<sup>2</sup>).

### 4. Results and Discussion

The simulations were conducted following the completion of the setup to generate comprehensive results. The analysis assessed the wind turbine's power generation capabilities, structural performance, and overall reliability under various operating conditions. In accordance with the Betz limit law, a wind turbine can extract a maximum of 59.3% of the available wind energy [22]. The performance evaluation emphasized measurements of torque, angular velocity, power, and power coefficient. These results were utilized to compare the shrouded wind turbine's performance under low wind conditions against that of conventional open rotor configurations (consisting of hub and blades only).

#### 4.1 Velocity Distribution Analysis

Velocity contours were generated to illustrate the spatial distribution of fluid velocity within the flow domain. These contours, obtained from CFD simulations, employed consistent color gradients to emphasize variations in velocity [23]. Fig. 3 presents the velocity contours for both configurations: (a) the shrouded wind turbine and (b) the conventional wind turbine. The results demonstrated a significant increase in air velocity following interaction with the shroud walls, leading to enhanced flow acceleration. Specifically, the shrouded configuration exhibited superior velocity enhancement, with increases of 11.6% at 4 m/s and 7.5% at 7 m/s relative to the open rotor design. Table 2 summarizes the velocity enhancement analysis, detailing the quantitative improvements across the tested wind speeds. This velocity augmentation was attributed to the Venturi effect induced by the shroud geometry, which functioned as a diffuser to accelerate flow through the rotor by reducing downstream pressure and increasing mass flux [24].

**Table 2** Velocity enhancement analysis

Wind Speed (m/s)	Velocity (m/s)		Enhancement (%)
	Shroud Wind Turbine	Without Shroud (Hub & blade only)	
4	8.84	7.92	11.6
7	10.57	9.83	7.5

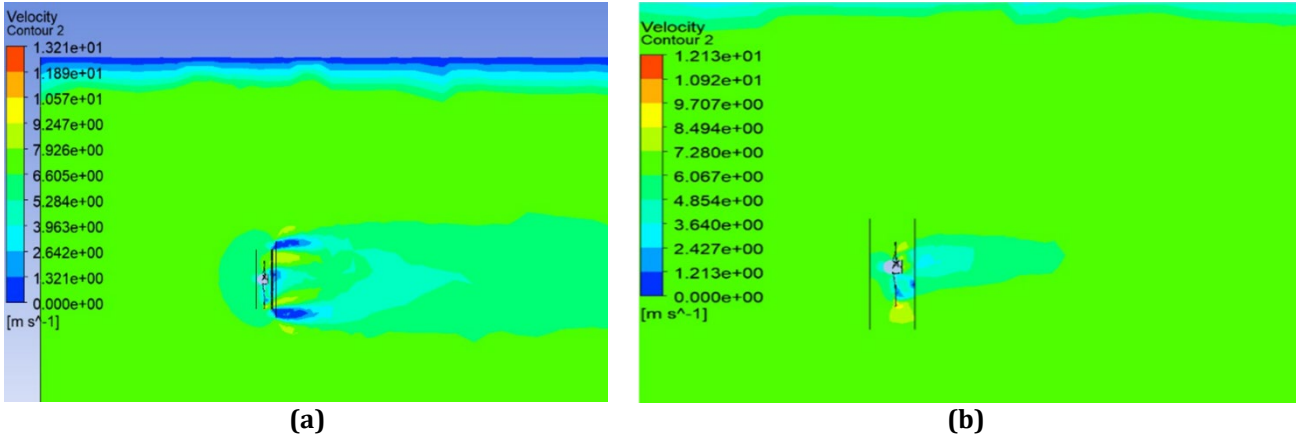


Fig. 3 Velocity contour. (a) Shrouded wind turbine; (b) Conventional wind turbine

### 4.2 Pressure Distribution Characteristics

Pressure contours provided useful information regarding the pressure distribution within the fluid system, highlighting the influence of geometric configurations on pressure patterns [25]. Fig. 4 displays the pressure contours for (a) the shrouded wind turbine and (b) the conventional wind turbine. The analysis indicated that the shrouded wind turbine experienced lower pressure levels compared to the conventional design. Table 3 provides a detailed comparison of pressure values on the wind turbine surfaces under the tested conditions. This pressure reduction aligned with Bernoulli's principle, wherein the increased velocity within the shroud resulted in decreased static pressure, thereby promoting enhanced mass flow through the rotor disk [26].

Table 3 Pressure on wind turbine

Wind Speed (m/s)	Pressure (Pa)	
	Shrouded Wind Turbine	Open Rotor (Hub & blade only)
4	23.1	25.01
7	25.24	33.82

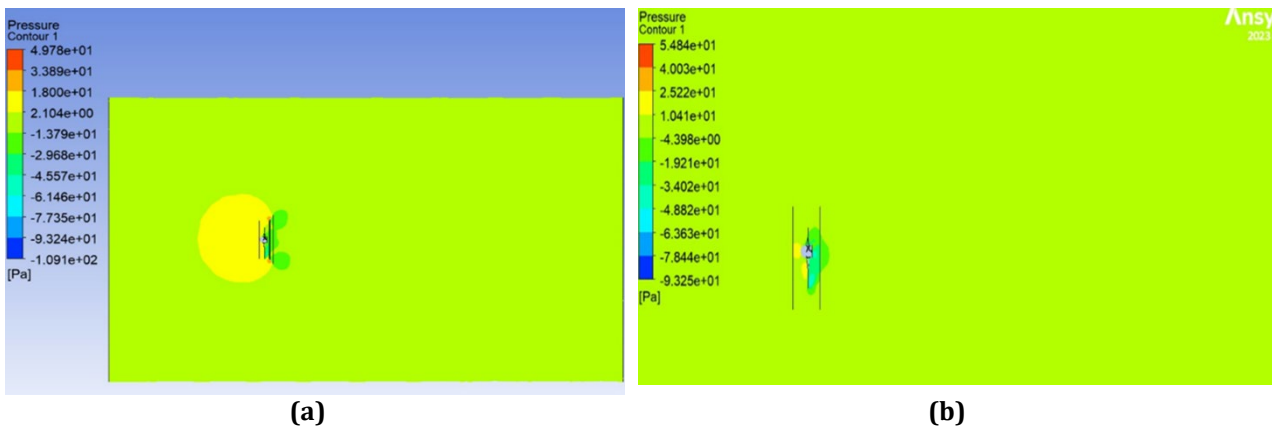


Fig. 4 Pressure contour. (a) Shrouded wind turbine; (b) Conventional wind turbine

### 4.3 Torque Generation Analysis

Shrouded wind turbine designs were developed to achieve superior performance relative to conventional open rotor configurations [27]. Torque characteristics were influenced by design specifications and operating conditions. Fig. 5 illustrates the relationship between torque and wind speed for both the shrouded and conventional turbines. The shrouded configuration consistently produced higher torque values across the tested wind speeds. Table 4 presents the torque data, showing values ranging from 1.13 N·m to 2.26 N·m for the shrouded turbine and 0.96 N·m to 2.15 N·m for the conventional design at wind speeds of 4 m/s to 7 m/s. This enhancement in torque was linked to the improved airflow control provided by the shroud, which optimized flow direction and minimized negative torque effects [28].

**Table 4** Torque

Wind Speed (m/s)	Torque (N-m)	
	Shrouded Wind Turbine	Open Rotor (Hub & blade only)
4	1.1302	0.9647
7	2.256	2.1484

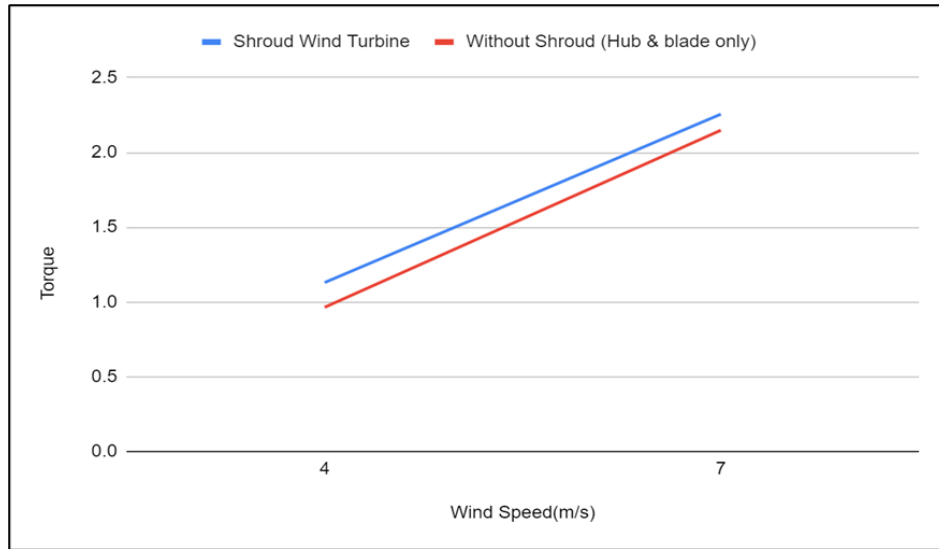


**Fig. 5** Torque vs. wind speed

#### 4.4 Power Coefficient Performance

The power coefficient ( $C_p$ ) served as a critical parameter for assessing the efficiency of wind turbines in converting kinetic energy from wind into mechanical power [29]. Various factors, including blade design, aerodynamic efficiency, rotor properties, and wind-turbine interaction dynamics, influenced the power coefficient. Fig. 6 depicts the power coefficient as a function of tip speed ratio (TSR) for both configurations. The shrouded wind turbine exhibited higher  $C_p$  values at elevated tip speed ratios compared to the conventional open rotor design. Table 5 details the power coefficient values, ranging from 0.139 to 0.052 for the shrouded configuration and 0.118 to 0.049 for the conventional design across TSR values from 1.1 to 1.9. Both designs operated well within the theoretical Betz limit of 0.594 [22]. The similar performance trends for both turbines, with increasing power coefficients, suggested that neither design achieved peak energy extraction at the tested tip speed ratios [30].

**Table 5** Power coefficient,  $C_p$

Wind Speed (m/s)	Power Coefficient ( $C_p$ )	
	Shrouded Wind Turbine	Shroud (Hub & blade only)
4	0.139	0.118
7	0.052	0.049

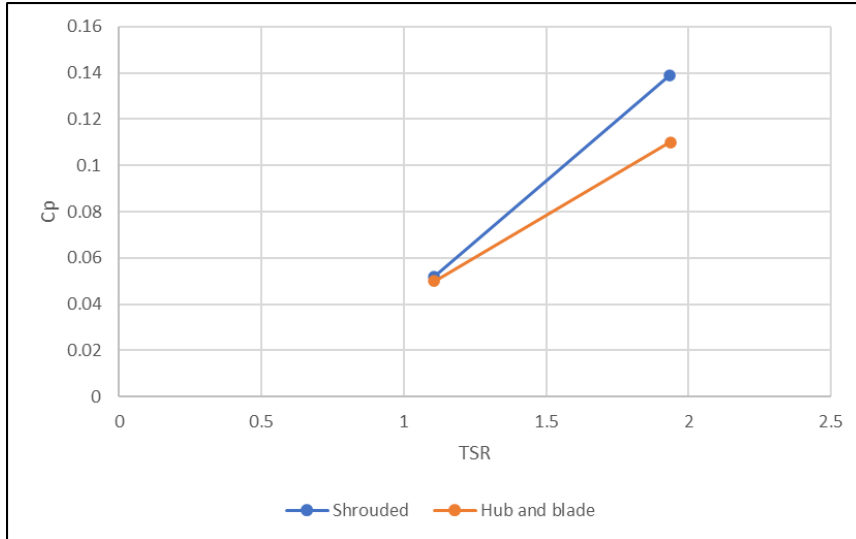


Fig. 6 CP vs TSR

### 4.5 Power Generation Comparison

Power generation constituted the primary objective of wind turbine design [31]. Multiple factors, such as wind speed, turbine characteristics, and system efficiency, affected power output. Power calculations were performed using equations (3) and (4). Fig. 7 shows the power output versus wind speed for shrouded and conventional turbines. The shrouded wind turbine demonstrated superior power extraction compared to the conventional open rotor design. Table 6 outlines the power generation analysis, with outputs ranging from 10.94 W to 21.83 W for the shrouded configuration and 9.34 W to 20.79 W for the conventional design across wind speeds of 4 m/s to 7 m/s. The power enhancement was more pronounced at lower wind speeds, achieving a 17.1% improvement at 4 m/s compared to 5.0% at 7 m/s. This improved performance validated the shroud's effectiveness in increasing power generation through enhanced wind speed acceleration [32].

Table 6 Power generation analysis

Wind Speed (m/s)	Power (w)		Enhancement (%)
	Shrouded Wind Turbine	Open Rotor (Hub & blade only)	
4	10.94	9.34	17.1
7	21.83	20.79	5.0

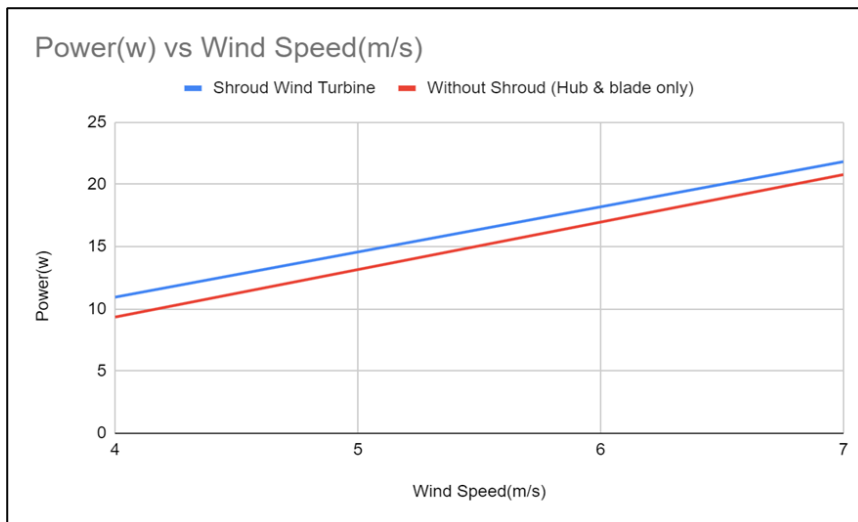


Fig. 7 Power vs. wind speed

## 5. Conclusion

This comprehensive study successfully examined an innovative approach for more effective wind power harnessing through shrouded wind turbine technology under low wind speed conditions. The research methodology employed the k- $\omega$  (SST) turbulence model for computational fluid dynamics analysis, and comprehensive results were obtained through the systematic integration of SolidWorks for design development and ANSYS Fluent for performance simulation. The primary objective of developing and analyzing a conceptual design for a shrouded wind turbine optimized for low wind speed conditions ranging from 4 to 7 m/s was successfully achieved. Through extensive CFD simulations, the proposed wind turbine's aerodynamic performance was thoroughly evaluated across multiple critical parameters, including power coefficient, tip speed ratio, velocity distribution, pressure characteristics, torque generation, and power output capabilities. The comparative analysis between shrouded and conventional open rotor configurations offered helpful information about the effectiveness of shroud implementation for low wind speed applications. The investigation showed that the shrouded configuration significantly outperformed conventional open rotor designs in terms of performance. The shrouded wind turbine demonstrated superior power coefficient values at elevated tip speed ratios, with the power generation showing a remarkable enhancement of 17.1% at 4 m/s windspeed and a 5.0% improvement at 7 m/s. These improvements were directly attributed to the enhanced velocity characteristics achieved through the shroud design, which increased air velocity by 11.6% at 4 m/s and 7.5% at 7 m/s compared to the open rotor configuration. The velocity augmentation was primarily caused by the Venturi effect created by the shroud geometry, which effectively accelerated the wind flow through the rotor disk area. The aerodynamic analysis further revealed that the shrouded design experienced lower static pressure compared to the conventional configuration, consistent with Bernoulli's principle, where increased velocity results in reduced pressure. This pressure differential facilitated enhanced mass flow through the rotor, contributing to improved energy extraction efficiency. Additionally, the torque generation analysis demonstrated that the shrouded configuration produced higher torque values across all tested wind speeds, ranging from 1.13 to 2.26 N·m compared to 0.96 to 2.15 N·m for the conventional design. This torque enhancement was attributed to the improved airflow control provided by the shroud, which optimized flow direction and reduced negative torque effects. The research findings conclusively demonstrated the significant benefits and practical viability of shrouded wind turbine technology for low wind speed applications. The shrouded design effectively addressed the fundamental challenge of energy extraction efficiency in low wind speed environments, making wind energy more accessible in regions previously considered unsuitable for conventional wind turbine installations. This study contributes substantially to the advancement of wind turbine design and optimization methodologies, providing a foundation for developing highly efficient and economically viable wind energy systems specifically tailored for low wind speed conditions. The results support the potential for broader implementation of shrouded wind turbine technology in distributed energy generation systems, particularly in urban and rural areas characterized by moderate wind resources.

## Acknowledgement

This research was conducted with the support of the Faculty of Mechanical and Manufacturing Laboratories at Universiti Tun Hussein Onn Malaysia (UTHM). The computational resources provided by UTHM were instrumental in conducting simulations for this study.

## Conflict of Interest

Authors declare that there is no conflict of interest regarding the publication of the paper.

## Author Contribution

*The authors confirm their contribution to the paper as follows: **study conception and design:** Syed Nazim Syed Ahmad, Nurhayati Rosly; **data collection:** Syed Nazim Syed Ahmad; **analysis and interpretation of results:** Syed Nazim Syed Ahmad, Nurhayati Rosly; **draft manuscript preparation:** Syed Nazim Syed Ahmad, Nurhayati Rosly. All authors reviewed the results and approved the final version of the manuscript.*

## References

- [1] M. O. L. Hansen, *Aerodynamics of Wind Turbines*, 3rd ed. London: Earthscan, 2015.
- [2] K. Adeyeye, N. Ijumba, and J. Colton, "Exploring the environmental and economic impacts of wind energy: a cost-benefit perspective," *International Journal of Sustainable Development and World Ecology*, vol. 27, no. 8, pp. 718–731, Nov. 2020, <https://doi.org/10.1080/13504509.2020.1768171>

- [3] G. Msigwa, J. O. Ighalo, and P. S. Yap, "Considerations on environmental, economic, and energy impacts of wind energy generation: Projections towards sustainability initiatives," *Science of the Total Environment*, vol. 849, Nov. 2022, <https://doi.org/10.1016/j.scitotenv.2022.157755>
- [4] N. Aslam Bhutta, M. F. Akhtar, A. Maqsood, S. Ahsan, S. Farooq, and M. A. Nawaz, "Technical and performance assessments of wind turbines in low wind speed areas using numerical, metaheuristic and remote sensing procedures," *Applied Energy*, vol. 356, p. 122393, Feb. 2024, <https://doi.org/10.1016/j.apenergy.2023.122393>
- [5] T. Wilberforce, A. G. Olabi, E. T. Sayed, A. H. Alalmi, and M. A. Abdelkareem, "Wind turbine concepts for domestic wind power generation at low wind quality sites," *Journal of Cleaner Production*, vol. 394, p. 136137, Mar. 2023, <https://doi.org/10.1016/j.jclepro.2023.136137>
- [6] M. R. Islam, R. Saidur, and N. A. Rahim, "Assessment of wind energy potentiality at Kudat and Labuan, Malaysia using Weibull distribution function," *Energy*, vol. 36, no. 2, pp. 985–992, 2011, <https://doi.org/10.1016/j.energy.2010.12.011>
- [7] D. H. Didane, N. Rosly, M. F. Zulkafli, and S. S. Shamsudin, "Performance investigation of a small Savonius rotor," *International Journal of Energy Research*, vol. 44, no. 12, pp. 9309–9316, Sep 2020, <https://onlinelibrary.wiley.com/doi/full/10.1002/er.4874>
- [8] J. A. Oliveira and Á. F. Flores Filho, "Performance evaluation of a stator modular ring generator for a shrouded wind turbine," *Energies*, vol. 14, no. 1, Jan. 2021, <https://doi.org/10.3390/en14010067>
- [9] P. Nithya Kalyani and B. V. S. S. S. Prasad, "Shrouded wind turbines: a critical review on research and development," *International Journal of Ambient Energy*, vol. 43, no. 1, pp. 8527–8546, 2022, <https://doi.org/10.1080/01430750.2022.2102064>
- [10] M. Nasrul and I. Rizianiza, "Shrouded wind turbine for low wind speed," *IOP Conference Series: Materials Science and Engineering*, vol. 1034, no. 1, p. 012042, Feb. 2021, <https://doi.org/10.1088/1757-899X/1034/1/012042>
- [11] A. Alaimo, A. Esposito, A. Messineo, C. Orlando, and D. Tumino, "3D CFD analysis of a vertical axis wind turbine," *Energies* vol. 8, no. 4, pp. 3013–3033, 2015, <https://doi.org/10.3390/en8043013>
- [12] T. Burton, N. Jenkins, D. Sharpe, and E. Bossanyi, *Wind Energy Handbook*, 2nd ed. Chichester, UK: John Wiley & Sons, 2011
- [13] J. F. Manwell, J. G. McGowan, and A. L. Rogers, *Wind Energy Explained: Theory, Design and Application*, 2nd ed. Chichester, UK: John Wiley & Sons, 2009.
- [14] A. G. Refaie, H. S. A. Hameed, M. A. A. Nawar, Y. A. Attai, and M. H. Mohamed, "Comparative investigation of the aerodynamic performance for several Shrouded Archimedes Spiral Wind Turbines," *Energy*, vol. 239, Jan. 2022, doi: <https://doi.org/10.1016/j.energy.2021.122295>
- [15] Y. Chen, D. Wu, Y. Yu, and W. Gao, "An improved theory in the determination of aerodynamic damping for a horizontal axis wind turbine (HAWT)," *Journal of Wind Engineering and Industrial Aerodynamics*, vol. 213, Jun. 2021, doi: <https://doi.org/10.1016/j.jweia.2021.104619>
- [16] A. L. Raveendran and B. Bala, "Comprehensive analysis with enhanced resolution of HAWT blade using CFD," *Walailak Journal of Science and Technology*, vol. 18, no. 17, Sep. 2021, <https://doi.org/10.48048/wjst.2021.23301>
- [17] N. Bournival, V. Sicot, S. Loonen, P. Devinant, and A. Halimi, "Characterization of aerodynamic performance of wind-lens turbine using high-fidelity CFD simulations," *Frontiers in Energy*, vol. 15, pp. 795–810, 2021, doi: <https://doi.org/10.1007/s11708-020-0713-0>
- [18] A. Alkhabbaz, H. S. Yang, W. Tongphong, and Y. H. Lee, "Impact of compact diffuser shroud on wind turbine aerodynamic performance: CFD and experimental investigations," *International Journal of Mechanical Sciences*, vol. 216, Feb. 2022, <https://doi.org/10.1016/j.ijmecsci.2021.106978>
- [19] A. Zhang et al., "A Robust and Efficient CFD Approach for Horizontal-Axis Wind Turbine Performance Prediction", *Journal of Marine Science and Engineering*, vol. 10, no. 9, Art. 1243, 2022, doi: <https://www.mdpi.com/2077-1312/10/9/1243>
- [20] C. C. Voigt, D. Russo, V. Runkel, and H. R. Goerlitz, "Limitations of acoustic monitoring at wind turbines to evaluate fatality risk of bats," *Mammal Review*, vol. 51, no. 4, pp. 559–570, Oct. 2021. doi: <https://onlinelibrary.wiley.com/doi/10.1111/mam.12248>

- [21] K. Oukassou, S. El Mouhsine, A. El Hajjaji, and B. Kharbouch, "Comparison of the power, lift and drag coefficients of wind turbine blade from aerodynamics characteristics of NACA0012 and NACA2412," *Procedia Manufacturing*, vol. 32, pp. 983–990, 2019, doi: <https://www.sciencedirect.com/science/article/pii/S2351978919303506>
- [22] N. Gopinath et al., "The Betz limit and the corresponding thermodynamic limit," *Wind Engineering*, vol. 145, pp. 10–21, 2022, <https://doi.org/10.1177/0309524X221130109>
- [23] A. Li, M. Gaunaa, G. R. Pirrung, A. Meyer Forsting, and S. G. Horcas, "How should the lift and drag forces be calculated from 2-D airfoil data for dihedral or coned wind turbine blades?" *Wind Energy Science*, vol. 7, no. 4, pp. 1341–1365, Jul. 2022, doi: <https://doi.org/10.5194/wes-7-1341-2022>
- [24] R. Bontempo and M. Manna, "On the potential of the ideal diffuser augmented wind turbine: an investigation by means of a momentum theory approach and of a free-wake ring-vortex actuator disk model," *Energy Conv. Manag.*, vol. 213, Art. 112794, 2020. Doi: <https://doi.org/10.1016/j.enconman.2020.112794>
- [25] M. Rivarolo, A. Freda, and A. Traverso, "Test campaign and application of a small-scale ducted wind turbine with analysis of yaw angle influence," *Appl. Energy*, vol. 279, Art. 115850, 2020. [Online]. Available: <https://doi.org/10.1016/j.apenergy.2020.115850> D. Zhao, N. Han, E. Goh, J. Cater, and A. Reinecke, "General introduction to wind turbines," *Wind Turbines and Aerodynamics Energy Harvesters*, Elsevier, 2019, pp. 1–20. doi: <https://doi.org/10.1016/j.apenergy.2020.115850>
- [26] M. A. R. Yass, R. Majeed Rasheed, and A. Hamad Muhiesen, "Contribution of lift-to-drag ratio on power coefficient of HAWT blade for different cross-sections," *Open Engineering*, vol. 12, no. 1, pp. 716–728, Jan. 2022, doi: <https://doi.org/10.1515/eng-2022-0324>
- [27] Y. Ohya and T. Karasudani, "A shrouded wind turbine generating high output power with wind-lens technology," *Energies*, vol. 3, no. 4, pp. 634–649, Mar. 2010. Doi: <https://doi.org/10.3390/en3040634>
- [28] F. Hilewit and J. Lazaro, "Power coefficient measurements of a novel vertical axis wind turbine," *Energy Science & Engineering*, vol. 7, no. 2, pp. 614–625, 2019. Doi: <https://doi.org/10.1002/ese3.412>
- [29] J. Dai, Y. Tang, Q. Wang, P. Jiang, and Y. Hou, "An Extended SFR Model with High Penetration Wind Power Considering Operating Regions and Wind Speed Disturbance," *IEEE Access*, vol. 7, pp. 103416–103426, 2019, doi: <https://doi.org/10.1109/ACCESS.2019.2930807>
- [30] O. Summerfield-Ryan and S. Park, "The power of wind: The global wind energy industry's successes and failures," *Ecological Economics*, vol. 210, Aug. 2023, doi: <https://doi.org/10.1016/j.ecolecon.2023.107841>
- [31] O. Carranza Castillo et al., "Comparison of power coefficients in wind turbines considering the tip speed ratio and blade pitch angle," *Energies*, vol. 16, no. 6, Art. 2774, Mar. 2023. Doi: <https://doi.org/10.3390/en16062774>
- [32] A. Alkhabbaz et al., "Impact of compact diffuser shroud on wind turbine aerodynamic performance: CFD and experimental investigations," *International Journal of Mechanical Sciences*, vol. 216, Art. 106978, Feb. 2022. Doi: <https://doi.org/10.1016/j.ijmecsci.2021.106978>